Figure S1

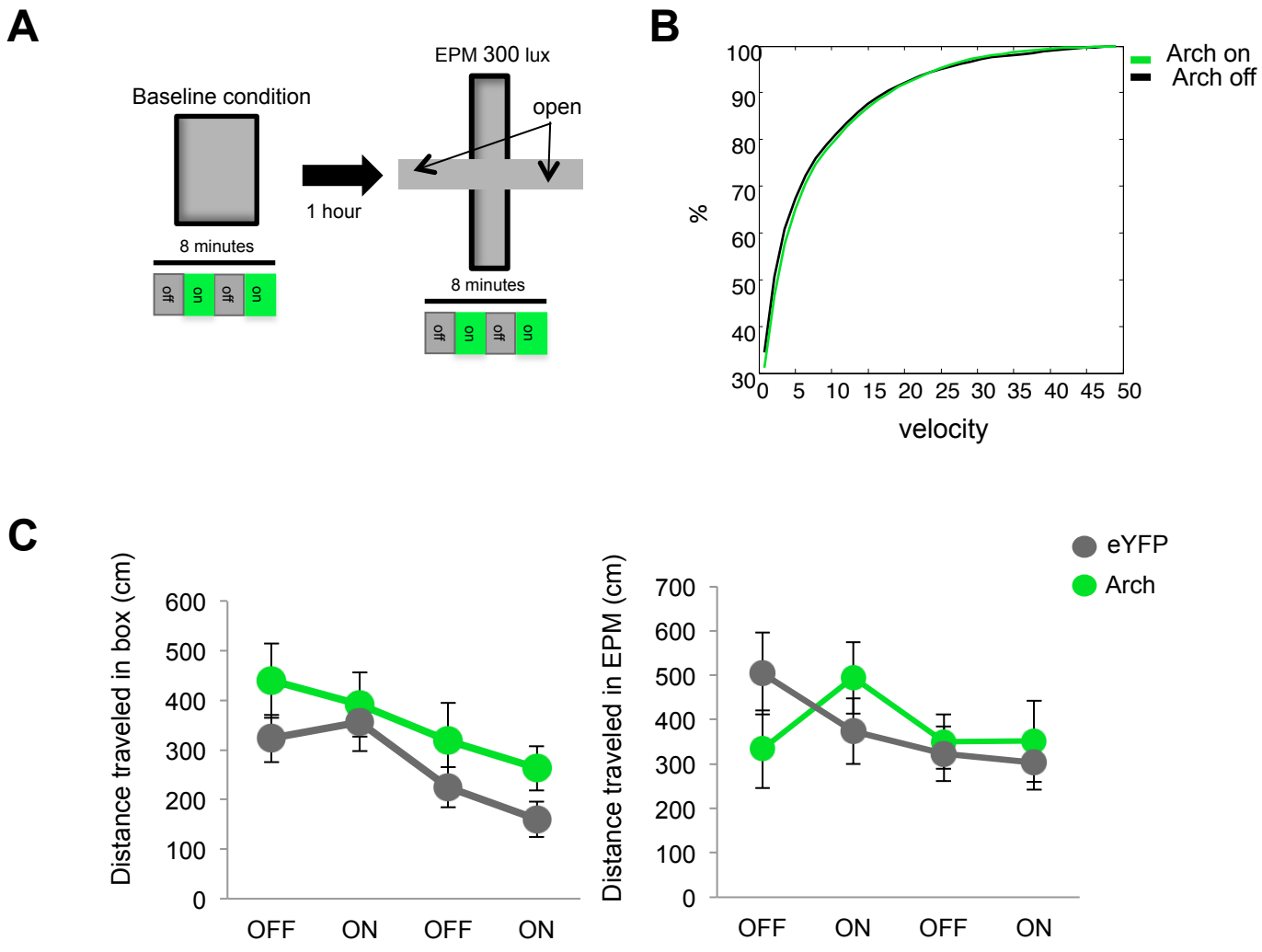

Figure S1, related to Figure 1 : **Inhibition of vHPC input to the mPFC does not affect locomotion.** (**A**) Diagram of behavioral protocol. Locomotion was measured in both a familiar box (left) and the elevated plus maze (right), with 8 minutes of exposure to each. Laser illumination of bilateral vHPC terminals in the mPFC was delivered in two minute epochs, alternating with no illumination. **(B)** Cumulative histograms of average velocity during bilateral terminal inhibition for Arch expressing mice (n=9). **(C**) Effects of terminal inhibition on distance traveled in the baseline box (left), and in the EPM (right) in Arch- and eYFP-expressing mice (n=10 and n=9, respectively). Data are presented as mean +/– SEM throughout, except where otherwise noted.

Figure S2

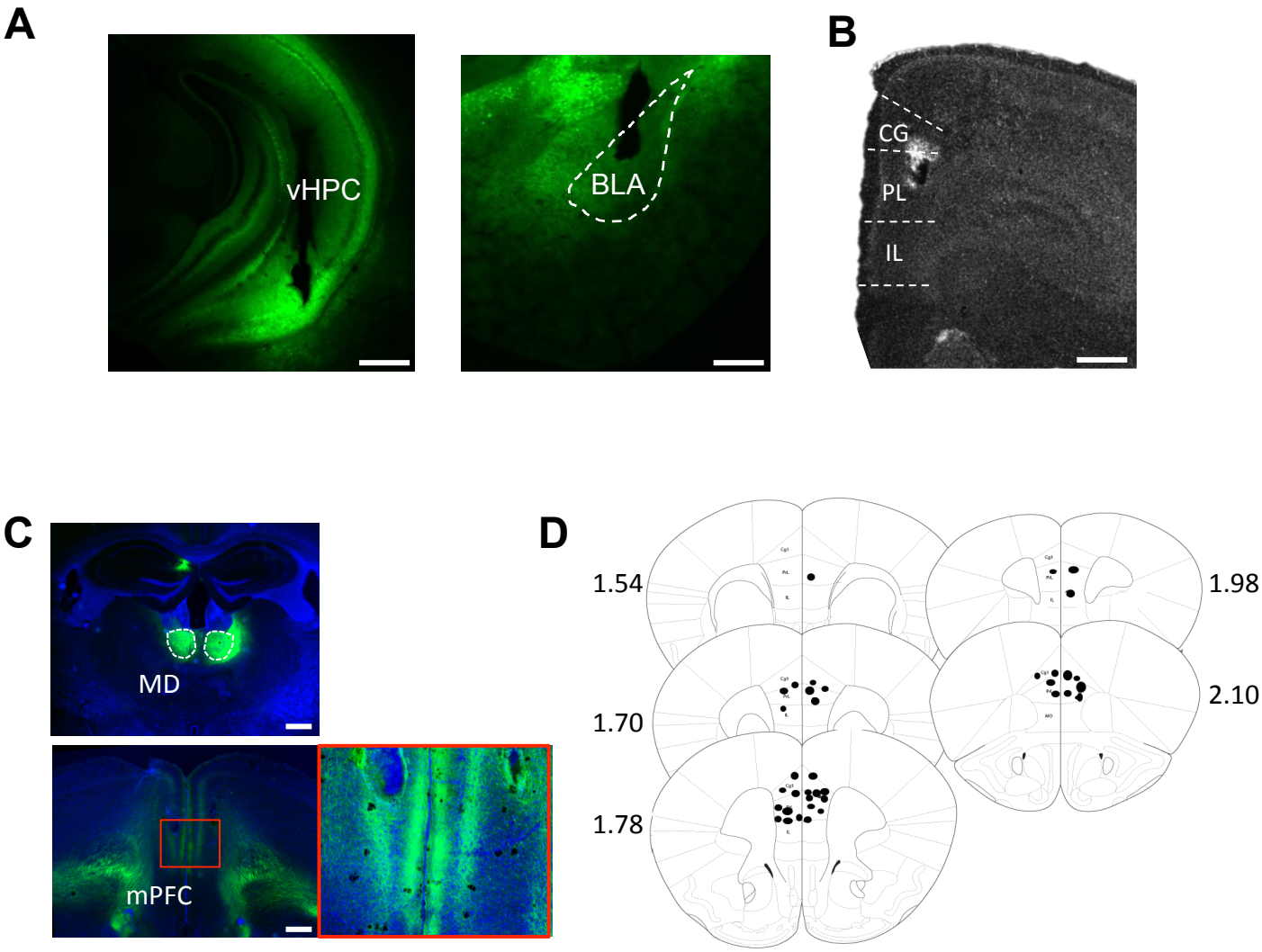

Figure S2, related to Figure 1: **Virally-mediated expression and electrode placement.** (**A**) Representative electrode locations for LFP wires implanted in the vHPC (left) and BLA (right). Green color is eYFP flourescence. White scale bar is 500 um for mPFC and vHPC and 100 um for BLA (**B**) Representative stereo-optrode location in the mPFC, imaged with DAPI (CG: cingulate cortex, PL: prelimbic cortex, IL: infralimbic cortex). (**C**) eYFP-tagged Arch flourescence in cells in the mediodorsal thalamus (MD, top) and terminals in the mPFC (bottom), after MD viral infection. Red square in bottom left indicates region shown magnified in bottom right. White scale bar is 0.5 mm. (**D**) Electrode placements in the mPFC, mostly located in the prelimbic (PL) cortex.

Figure S3

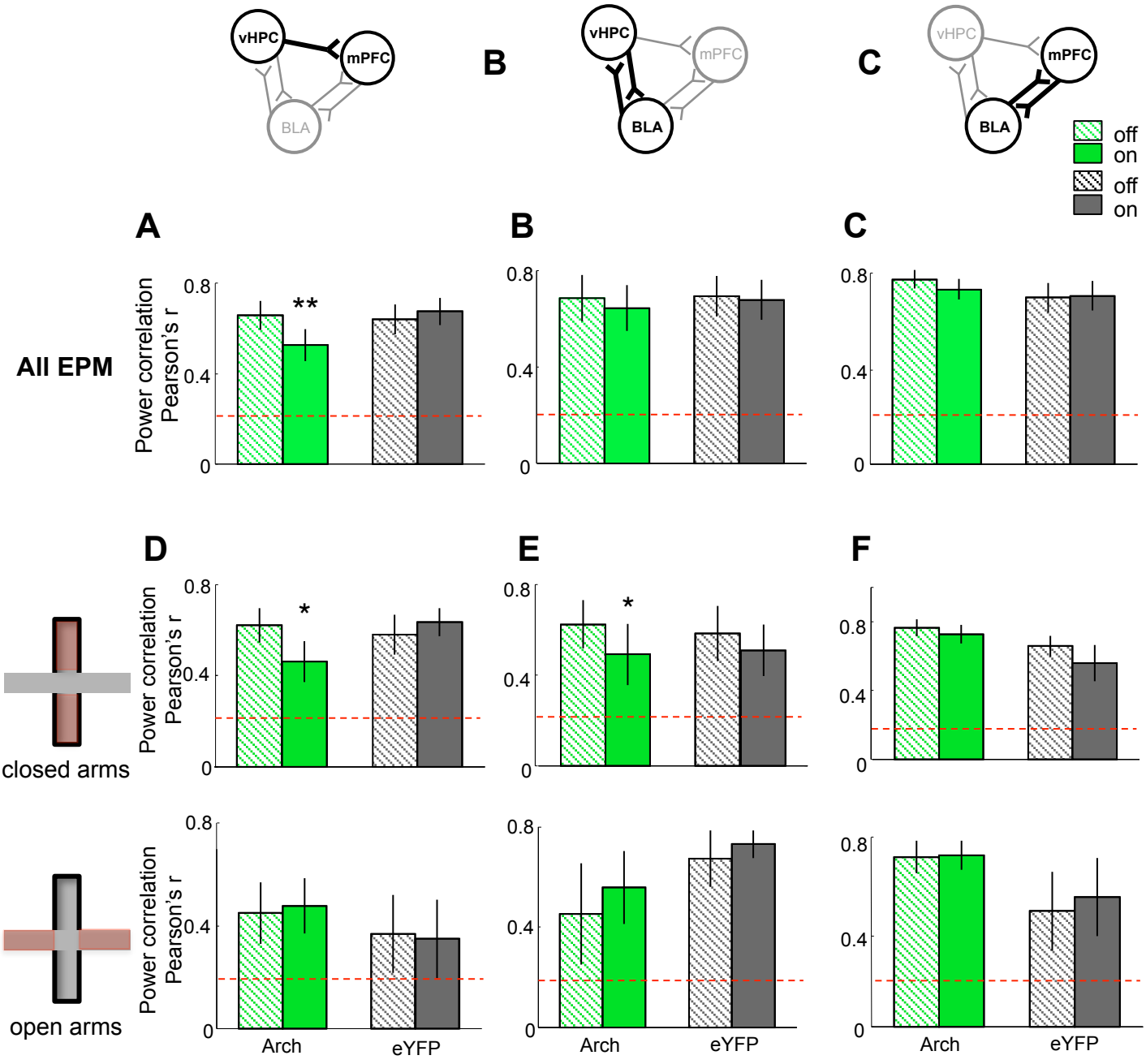

Figure S3, related to Figure 2: Inhibition of hippocampal-prefrontal input disrupts theta power correlation in a pathway-specific manner (**A-C**) Theta power correlations for vHPC-mPFC (**A**) (Arch n=10; eYFP n=11; **, $p < 0.01$ Wilcoxon sign-rank test); vHPC-BLA (**B**) (n=7 per group); and mPFC-BLA (**C**) (Arch n=7; eYFP n=6). (**D-F**) Theta power correlation calculated separately for data from the closed arms (top) and open arms (bottom) for the vHPC-mPFC (**D**) (*, p=0.0234, sign-rank); vHPC-BLA (**E**) (*, p=0.0413, sign rank) and the mPFC-BLA (**F**). Dashed red lines indicate critical value ($p<0.05$) for power correlations generated with shuffled data.

Figure S4

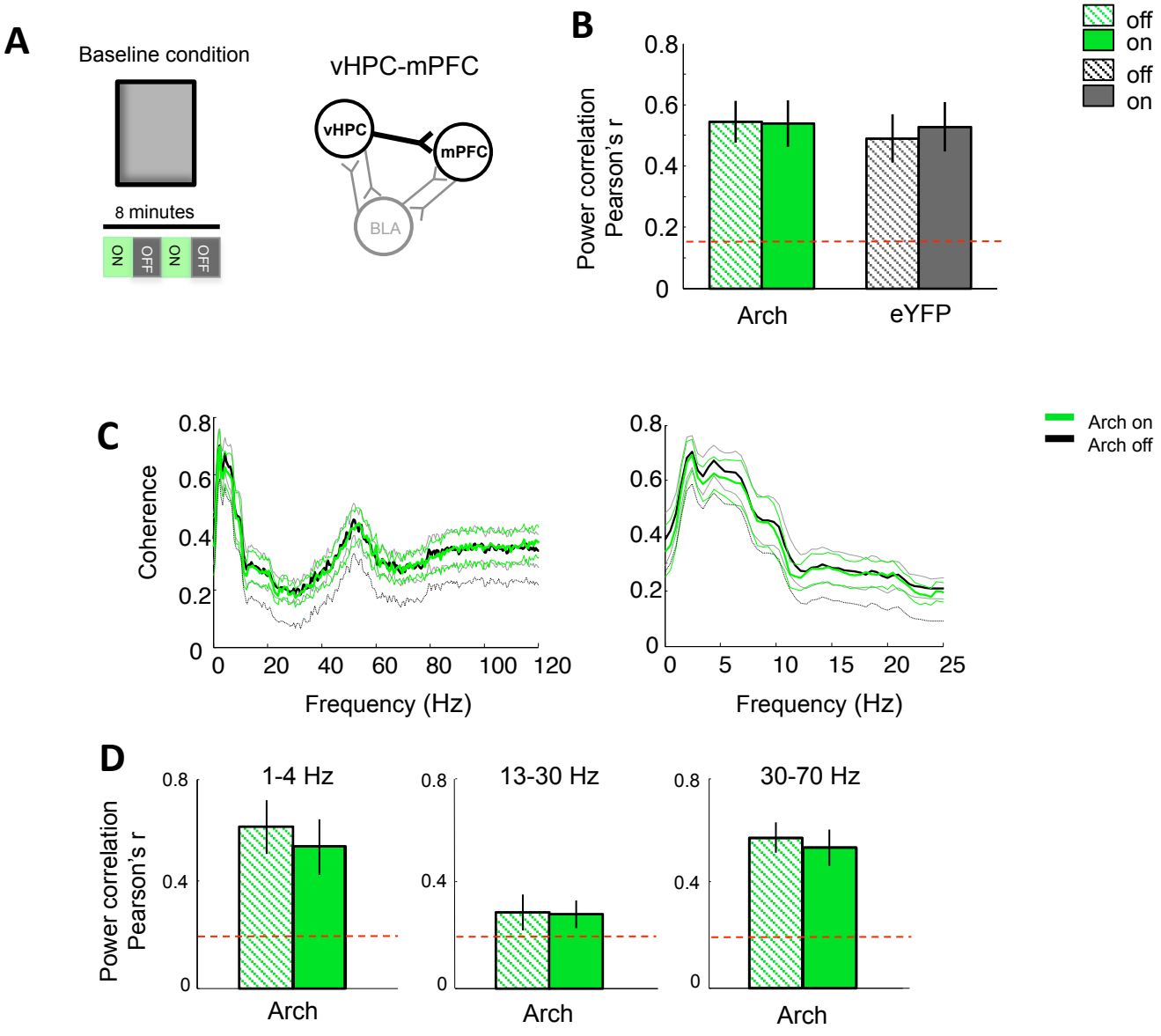

Figure S4, related to Figure 2: Inhibition of vHPC-mPFC pathway disrupts power synchrony in a task and frequency dependent manner (**A**) schematic of the behavioral experiment and the recorded sites. (**B**) Power correlation in the 4-12 Hz range for vHPC and mPFC in the baseline condition (n=10 for arch and n=11 for eYFP). (**C**) Coherence spectral between the vHPC and mPFC in the Arch group during the EPM (mean ± sem). Dashed lines 95% confidence interval. (**D**) Power correlations for vHPC and mPFC LFPs in the delta (1-4 Hz; Wilcoxon sign rank test p=0.13), beta (13-20 Hz) and slow gamma (30-70 Hz) frequency ranges during the EPM. Red lines in **B** and **D** indicate critical value ($p<0.05$) for power correlations generated with shuffled data.

Figure S5

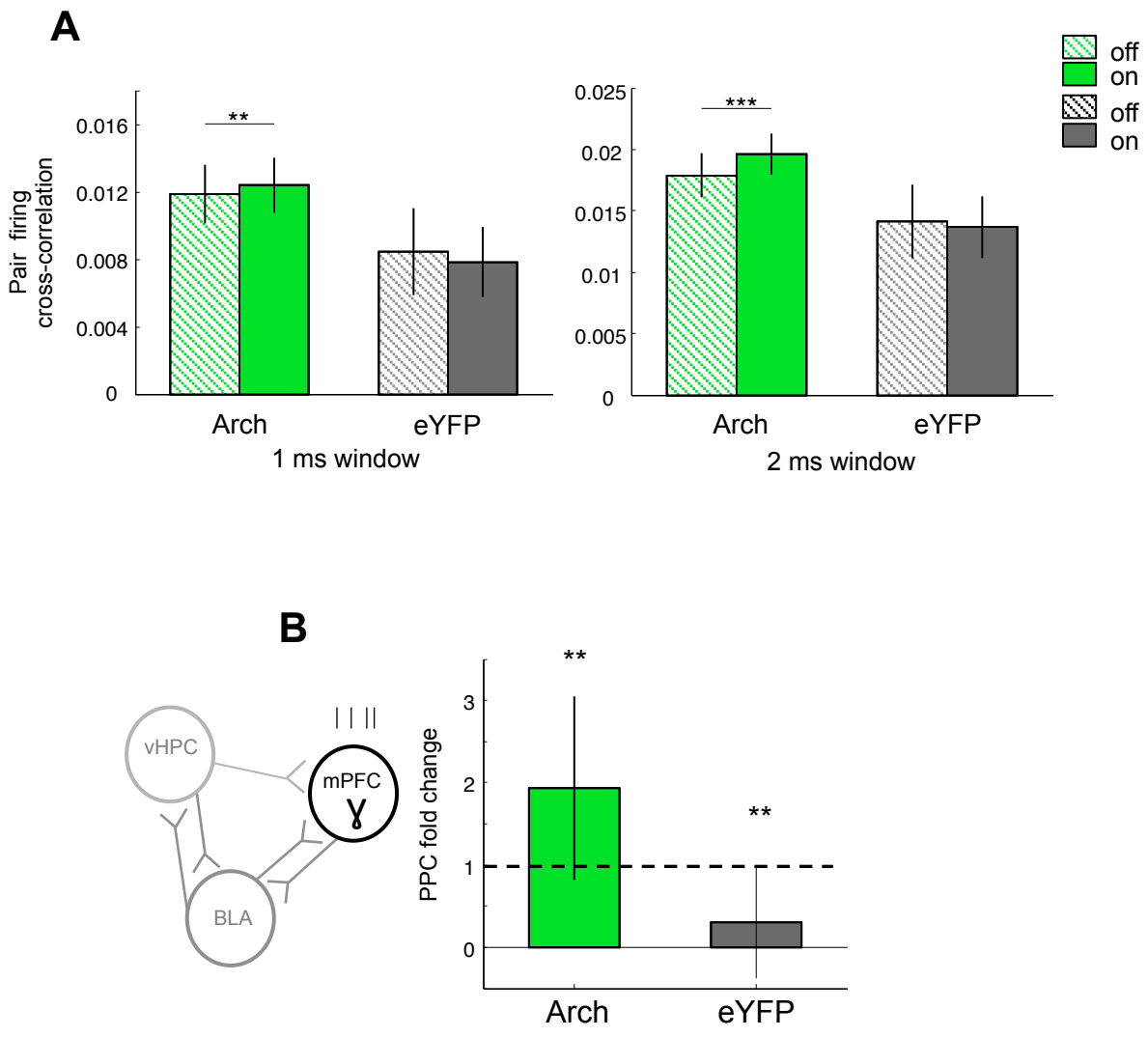

Figure S5, related to Figure 2: Inhibition of vHPC-mPFC pathway increases synchrony within the mPFC. (A) Cross-correlation of spikes during 1 ms window for simultaneously recorded pairs of mPFC single units during the EPM (Arch n=842 ***, p<0.01; eYFP n=416; p=0.26; Wilcoxon paired test). Cross-correlation of spikes during 2 ms window for mPFC simultaneously recorded single units during the EPM (Arch n=842, ***p<0.001; eYFP n=416 p=0.10; Wilcoxon paired test). **(B)** Fold change (ON/OFF) for phase locking strength to local fast gamma (Arch n=79 p<0.01; eYFP n=46 p<0.01; Wilcoxon one sample test). Dashed line is unity (no change).

Figure S6

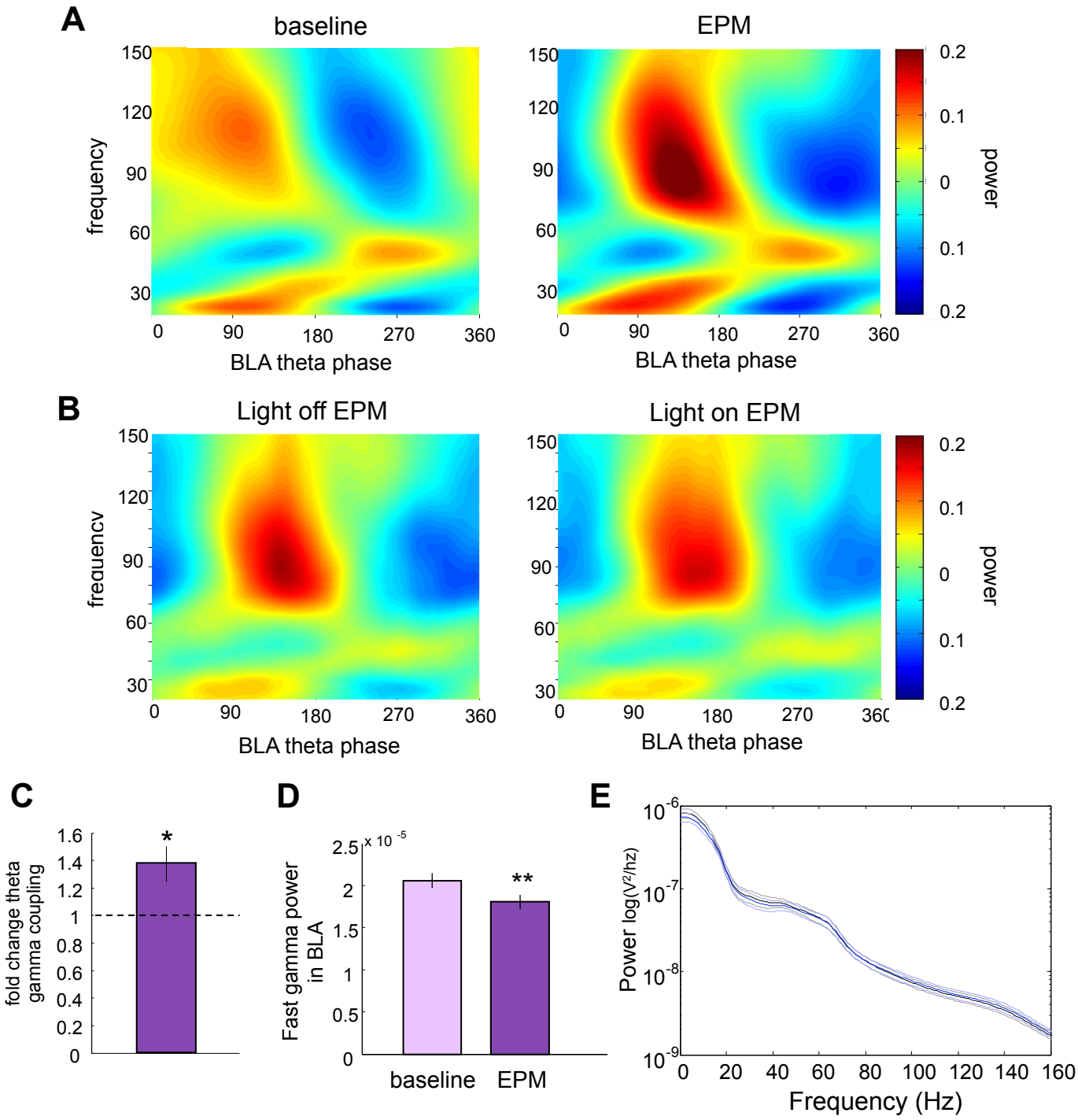

Figure S6, related to Figure 7: The EPM induces alterations in theta-gamma coupling and gamma power. (A) Example BLA comodulogram from the same electrode in the baseline condition (left) and in the EPM (right). **(B)** Averaged comodulograms for Arch animals in the closed arms of the EPM with the light off and the light on. (**C**) Fold change in theta-gamma coupling during the EPM vs baseline, as measured with MRL (n=19; *p<0.05; one sample Wilcoxon sign rank test). (**D**) Average fast famma power in the BLA during the baseline recording and the EPM (n=19, **p<0.01; paired Wilcoxon sign rank test). (**E**) Averaged BLA power spectra in the closed arms of the EPM for Arch injected animals (light off=black; light on=blue).

Figure S7

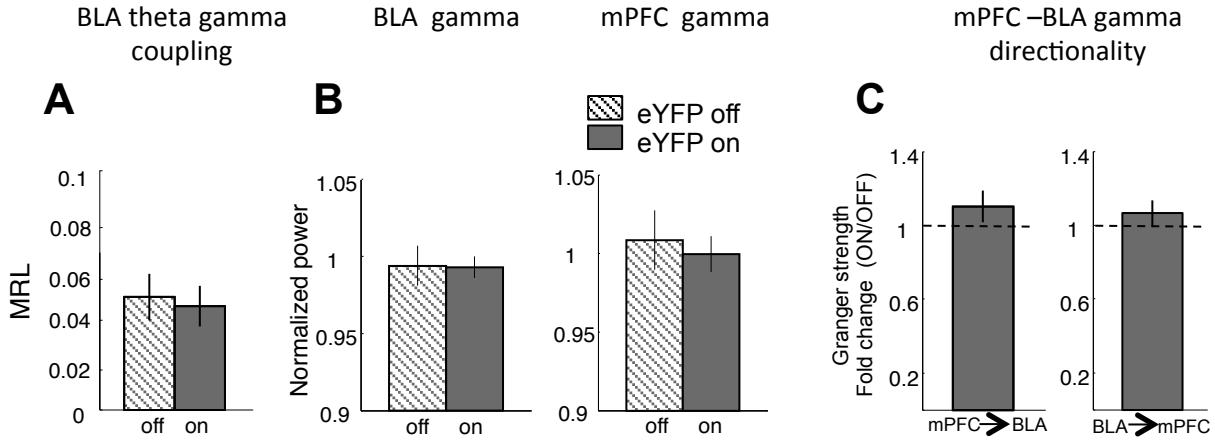

Figure S7, related to Figure 7: Illumination does not affect BLA or mPFC fast gamma measurements in eYFP animals. (A) BLA theta and fast gamma (70-120 Hz) coupling (n=9, p=0.25 Wilcoxon sign rank paired test). **(B)** Fast gamma power in BLA (p=0.36; Wilcoxon sign rank paired test) and mPFC (eYFP n=11, p=0.59) **(C)** Fold change in granger directionality strength in the mPFC to BLA direction (left) and the BLA to mPFC direction (right). Dashed lines indicate unity (no change).